Frequenz
63 (2009)
9–10

Implementation of ultra-wideband sensors for biomedical applications

F. Thiel, M. Helbig, U. Schwarz, C. Geyer, G. Rimkus, W. A. Kaiser, I. Hilger, M. Hein, J. Sachs, and F. Seifert

Abstract –With the ambitious aim to exploit the specific advantages of ultra-wideband (UWB) radio sensors for medical applications the project *ultraMEDIS* has been designed. The project focuses on the combination of UWB radar with magnetic resonance imaging, UWB radar based breast cancer detection, identification of various physiological signatures and the development of appropriate UWB antennas to accomplish these tasks.

Index Terms – Ultra-wideband radar, magnetic resonance imaging (MRI), breast cancer detection, MRI compatible antennas.

1 Introduction

Recent developments of semiconductor technologies, signal processing, and antenna design have intensified research of ultra-wideband (UWB) techniques for multiple applications. The benefits of a wide range of frequencies for simultaneous use centred at a sufficiently low frequency, low integral power, and mature circuit technologies form a promising basis for UWB sensor systems, where high resolutions in time and space and co-existence with narrow-band radio frequency (RF) systems can be exploited. Within a priority programme of the German Research Foundation (DFG) on UWB techniques for communication, localisation, and sensing (UKoLoS) [1] we have established a research project to exploit UWB sensing for medical applications (*ultraMEDIS*) [2] The project merges the interdisciplinary expertise of physicists, engineers, and biomedical scientists. Due to the ultra-low power signals involved, this approach is especially suitable for human medical applications. The technique permits non-invasive sensing with no potential risks, in contrast to catheter or X-ray techniques [3]. Furthermore, the project shall lead to a synergetic technological development of UWB radar combined with magnetic resonance imaging (MRI) [4], [5], to access innovative fields of applications such as UWB-navigated cardiac MRI [6], heart beat monitoring [7], [8], accurate modelling of electromagnetic wave propagation through heterogeneous, malignant and benign, biological tissues [9], [10] [11], and the fast and precise identification and localisation of breast cancer [11], [12], [13]. The paper is intended to give an illustrative insight into these different areas of research.

2 Biomedical Applications

2.1 Magnetic Resonance Imaging and UWB Radar

Magnetic resonance imaging (MRI) is the most important tool in modern cardiology and neuroscience. Due to the continuing improvements in spatial and temporal resolution in this imaging modality, great progress could be made in the field of brain science and cardiology. Nowadays, however, a point has been reached where further improvements in resolution is limited. The use of so called high- and ultra-high-field systems can overcome these limits and facilitate new findings about the human brain and the heart. Since signal to noise ratio in MR-imaging increases linearly with increasing static magnetic field the tendency towards higher fields is comprehensible. For imaging the heart, MRI is reliant on position information to acquire an image over multiple cardiac cycles by collecting segments of *k*-space at the same position in all contraction cycles. In standard clinical 1.5 T MRI systems electrocardiogram (ECG) triggering can be sufficiently applied for this task, for the variability of cardiac position (physiological noise) over several cycles can be regarded to be below the resolution of the MRI system (not regarding the measurement duration). With high and ultra-high field systems (3 T, 7 T, 9.4 T) entering clinical praxis and research, other non-invasive motion tracking techniques are required, since the resolution of these systems can only be exploited if cardiac contraction cycles with appropriate smaller variance are chosen (e. g. in a post-processing), especially in a free-breathing scenario. While penetrating into the human body, the UWB signal propagates in a three-dimensional manner and reflects the motion of a large area at a certain propagation time, e. g. the surface of the heart, which follows a cyclic highly non-linear motion. Therefore we proposed a combined MRI/UWB radar technique and have shown the feasibility of such an approach on phantoms and *in-vivo* (see Fig.1 left) [4]. Results from analytical and model based investigations on the electromagnetic wave propagation through stratified dielectric layers [9], such as the human thorax, inspired the investigation, weather UWB radar provides the mechanical deformation data from the myocardium and holds the potential to serve as a navigator technique as requested above. Our *in-vivo* experiments on volunteers of a combined MRI/UWB [6] and an ECG/UWB method [8] have shown, that the mechanical representation of the cardiac contraction provided by UWB radar varies dependent with the cardiac contour and the illuminated superficial part of the myocardium. The results are very satisfactory and prove the ability of UWB radar to monitor physiological events directly at their origin inside the body (s. Fig.1 right) and to identify landmarks a MR scanner can be triggered with. Optimization of data acquisition by the use of UWB antenna arrays to localize the motion in a focused area, will further improve the result.

2.2 Breast Surface Identification for UWB Breast Imaging

The dielectric constant of malignant breast-cancer, was found to be enhanced by a factor of 5 compared to benign breast tissue, in the frequency range 0.1…10 GHz [14]. Such a contrast provides a solid basis for the application of UWB techniques to medical tomography. Unfortunately UWB breast imaging is characterized by a very low signal-to-clutter ratio. Dominant skin reflection, which does not contribute to the imaging of the breast interior but which can mask tumour reflections, has to be removed. The non-planar geometry of the breast complicates this task enormously, because surface and interior reflections superimpose. Therefore, an exact identification of the breast surface is necessary. Based on an accurate knowledge of the breast surface and of the antenna

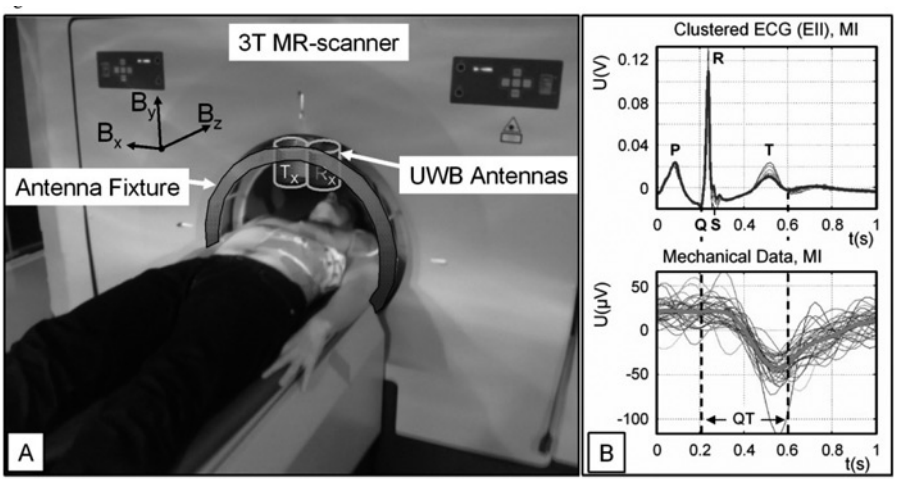

Fig. 1: *Left* **(A):** Typical set-up for a combined MRI/UWB measurement just outside the bore of PTB's 3-T MR scanner. *Right* **(B):** Results of a combined ECG/UWB radar experiment. *Upper right:* overlapped ECG epochs. *Lower right:* overlapped corresponding myocardial deformation reconstructed from sub-surface reflections of the thorax (depth ~ 5 cm, assuming a ε' ~ 60). The bold line indicates the mean signal. $B_z = 3$ T; B_x, $B_y << B_z$.

impulse response, an antenna position dependent skin reflection signal can be estimated and subtracted from the raw signal. Furthermore, knowledge of the surface geometry is essential to calculate the refraction angles, in order to image the interior of the breast based on migration techniques. The high resolution and high-speed UWB imaging method SEABED [15] represents a powerful approach for such surface detection problems. The practical applicability of the original algorithm [15] to our problem is limited because of the inherent planar scanning scheme. An adequate identification of lateral breast regions based on planar scanning over the chest would require very long scan distances. For this reason, the original approach was extended and tested by the authors [11], [12] towards non-planar scanning. Based on a three-dimensional antenna movement and scan shape dependent coordinate transforms this extension allows nearly arbitrary scanning schemes. The main challenges are the exact spatial detection of the wave fronts and their proper derivative. For the purpose of wave front detection we use an iterative super resolution algorithm. The resolutions of spatial scanning and radar signal sampling have to be carefully harmonized with each other in order to avoid derivative artefacts. Furthermore, we established thresholds of maximum feasible values, e.g. dependent on the antenna beam width. Fig.2 shows the UWB surface reconstruction using a double-ridged horn antenna (gain about 10 dBi) and a laser reference measurement of an artificial female torso which was filled with tissue equivalent phantom material (bandwidth used: 12 GHz). The histogram of the Euclidean distances between the UWB identified surface points and the respective nearest laser identified surface point demonstrates aberrations on the scale of millimetres. The aberrations to the real body surface are probably lower [16]. The results underline that the task of breast cancer detection requires a high bandwidth. In spite of their stronger attenuation, higher frequencies (>5 GHz) are essential for short skin reflections in order to facilitate the wave front detection and in order to avoid masking of reflections from tumours adjacent to the breast surface.

2.3 UWB Antennas for Biomedical Applications

The preceding paragraphs describe two different approaches for the use of UWB microwave signals in biomedical applications requiring specially designed antennas. For the specific case of combined MRI/UWB radar applications, the focus was on directive antenna elements which would not be affected by the presence of the strong static and dynamic magnetic fields of the MR scanner (3 T and 50 T/s). This led to a double-ridged horn antenna (DRH) design, optimized for minimal electromagnetic induction and eddy current distribution. This goal was met by a consequent metallization reduction process: (i) limitation of the copper conductor thickness to 10 µm; (ii) reduction of conductor faces to a grid structure; and (iii) extraction of the horn sidewalls in *H*-plane. The total volume could be reduced by a factor of 240, nonetheless keeping proper radiation characteristics. The antenna provides a -10 dB VSWR bandwidth between 1.5 and 12 GHz, a homogeneous and almost frequency independent main lobe with an averaged Gain = 7 dBi and an impulse response well below 200 ps. In conclusion, no interactions between the MR scanner and the modified antenna could be observed. The resulting antenna [17] is shown in Fig.3a (aperture plane 48×70 mm^2, depth 67 mm). The challenge changes for breast cancer imaging. For a direct contact placement of an antenna array upon the breast, geometrically small antennas are required [18]. With regard to a sufficient signal penetration, we set the lower cut-off frequency to 1.5 GHz with a wavelength of 225 mm. The maximum bandwidth used amounts to 10 GHz. To reduce the resulting conventional antenna sizes of up to 130×90 mm^2 for the aperture plane, we introduced the use of high-dielectric materials for geometrical scaling of the dielectrically loaded antennas. Currently, two different materials with a permittivity of $\varepsilon' = 22 \pm 2$ were applied for different tasks. While acetone is used for antenna measurements because of its electrical, optical and liquid properties, a biocompatible compound of oil and gelatine is used as an antenna enclosing material for

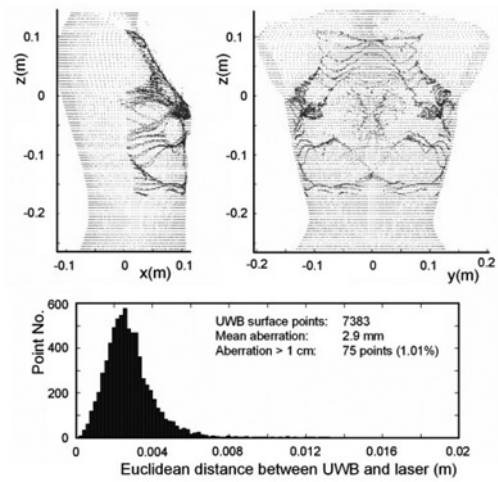

Fig. 2: UWB reconstruction (blue) of a female torso superimposing a reference measurement (red) by a laser distance meter (upper panels) and the aberration histogram between both (lower panel).

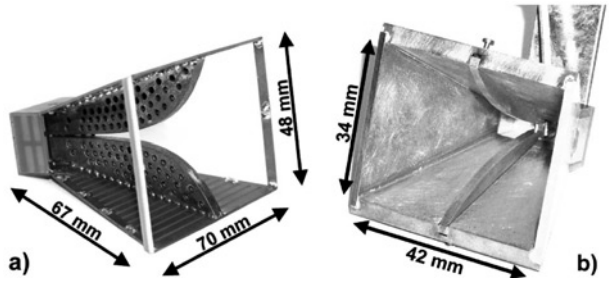

Fig. 3: MR-compatible double-ridged horn (DRH) antenna for a lower cut-off frequency of 1.5 GHz, fabricated from metallized dielectrics (left-hand panel) and a laboratory version of a DRH antenna with adjustable wings designed for immersion in acetone ($\varepsilon' = 22$, right-hand panel).

proband measurements. This resulted in a aperture size reduced by a factor of 8, still keeping the excellent impulse radiation capabilities, as shown in Fig.3b [5]. Beside the geometrical scaling, the use of dielectric material within antennas, enables an increased signal dynamic range of up to 25 dB due to reduced signal reflections at the skin surface as well as a more focused power density. This approach appears promising for contact-mode measurements, although the alternative approach based on remote electronical scans offers other advantages [5]. The upcoming work contains further miniaturized antennas based on ceramic materials with increased efficiency and more realistic array dimensions.

2.4 Physiological Signatures of UWB Signals

In order to build up suitable models for electromagnetic wave scattering in living tissue, empirical tests and measurements have to be undertaken. Furthermore, the feasibility of the proposed UWB sensing method in relation to diagnostic procedures, particularly of tumours in the breast and physiological signatures has to be carried out. Physiological signatures can be investigated by UWB signals, for a good differentiation in water content and accordingly in dielectric properties between non-hydrous (fat) and hydrous organs (muscle, liver, kidney) can be made [10], [18]. Many pathophysiological changes in humans are known to be associated with a change of water content. Hence UWB sensing potentially offers a broad spectrum of application in clinical diagnostics. Focusing the diagnosis of breast cancer, studies to characterise the permittivity of malignant and glandular tissue by dielectric spectroscopy in the frequency range of 1 GHz to 4 GHz were carried out using standard coaxial probes. Glandular tissue was modelled by bovine udder, malignant tissue by a VX-2 tumour which was implanted subcutaneously into a rabbit. First, the permittivity of a grown VX-2 tumour (32 cm^3) and the surrounding healthy tissue was determined *in-vivo*. When measuring the dielectric properties of tumour bearing animals, permittivity values are determined by the mixture of cancerous tissue, skin covering the tumour and the tumour's interior blood circulation (*in-vivo* cancerous tissue's dielectric values: ε'; $\varepsilon'' = 55-49$; $17-10$) (Fig. 4). In contrast, healthy tissue permittivity values were formed by the skin and normal connective and fatty tissue (healthy tissue's permittivity: ε'; $\varepsilon'' = 26-23$; $7-3$). Assessing the effect of blood circulation on permittivity the same tumour was also measured *post mortem*. In this case, the permittivity values were solely influenced by cancerous tissue and the skin covering the tumour. Accordingly the dielectric properties of the tumour decreased to values between ε'; $\varepsilon'' = 49-41$; $14-9$. In order to determine the permittivity of cancerous tissue only, the dissected tumour had to be measured. The permittivity values were found to be between ε'; $\varepsilon'' = 62-46$; $22-12$ (Fig. 4). The results show how permittivity is influenced by different tissue types and physiological parameters. However, when comparing different tissue types the respective experimental conditions have to be taken into account. Due to the fact, that tumours of the breast primarily originate from glandular tissue, the dielectric permittivity of gland was accordingly determined *ex vivo* at the glandular surface. Glandular tissue is very hydrous, thus being associated with a high permittivity (ε'; $\varepsilon'' = 57-47$; $18-14$). Comparing *ex vivo* malignant (ε' and $\varepsilon'' \approx 5.1$ and 2.01, respectively) and glandular tissues (ε' and $\varepsilon'' \approx 4.1$ and 2.6, respectively) (Fig. 4) the permittivity seems to be quite similar, implicating the need for further investigations focusing on improved resolution and data analysis.

3 Conclusion

Due to the strong co-operative research of the interdisciplinary *ultraMEDIS* consortium, our work has created a sound theoretical, experimental an technical basis, whereupon significant improvements in established clinical imaging modalities can be stated, as well as new screening techniques for breast cancer detection and physiological signature monitoring can be developed.

4 Acknowledgements

The authors are grateful to W. Hoffmann, F. Wojcik, D. Kreiseler, A. Schnabel, F. Petsch, and T. Lindel from PTB and to E. Hamatschek, M. Fritz, M. Kmec, R. Herrmann and K. Schilling at TU Ilmenau and P. Rauschenbach from MEODAT GmbH for helpful hints and technical support.

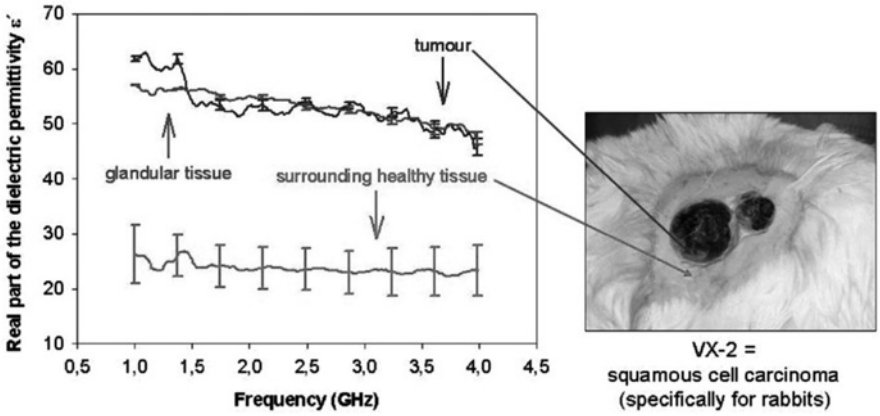

Fig. 4: Dielectric properties of biological tissues. The left panel shows the real part of the dielectric permittivity of glandular, cancerous and tumour surrounding healthy tissue. The right picture depicts the location of measuring points at the cancerous (VX-2 tumour) and the healthy tissue of a rabbit.

References

[1] (2008) The UKoLoS website. [Online]. Available: http://www.-emt.tu-ilmenau.de/ukolos/
[2] (2008) ultraMEDIS [Online]. Available: http://www-emt.tu-ilmenau.de/ukolos/sub_ultraMEDIS.php.
[3] J. Sachs, P. Peyerl, S. Wöckel, et al., Liquid and moisture sensing by ultra-wideband pseudo-noise sequence signals, Meas. Sci. Technol., vol. 18, pp. 1074–1088, (2007).
[4] F. Thiel, M. Hein, J. Sachs, U. Schwarz, F. Seifert, Combining MRI and ultra wideband radar: A new concept for multimodal biomedical imaging, Rev. Sci. Instrum., vol. 80, no. 1, (2009)
[5] U. Schwarz, F. Thiel, F. Seifert, R. Stephan, M. Hein, Ultra-Wideband Antennas for Combined Magnetic Resonance Imaging and UWB Radar Applications, Proc. IMS, p. 1433–1436, (2009)
[6] F. Thiel, M. Hein, J. Sachs, U. Schwarz, F. Seifert, Physiological signatures monitored by ultra-wideband-radar validated by magnetic resonance imaging, Proc. ICUWB 2008, pp. 105–108, (2008).
[7] F. Thiel, M. Hein, J. Sachs, U. Schwarz, T. Lindel, F. Seifert, Influence of strong static magnetic fields on myocardial mechanics: evaluation applying UWB radar, Proc. Intl. Soc. Mag. Reson. Med. (ISMRM), (2009).
[8] F. Thiel, M. Hein, U. Schwarz, and F. Seifert, Multimodal biomedical sensing applying ultra-wideband electromagnetic excitation, Proc. ICUWB 2009, (2009)
[9] F. Thiel and F. Seifert, Non-invasive probing of the human body with electromagnetic pulses: modeling of the signal path, J. Appl. Phys., vol.105, issue 4, 044904, ISSN 0021–8979, (2009)
[10] Geyer C, Helbig M, Schwarz U, et al., Image-based detection of water contents in tissue-modelling phantoms by ultra-wideband sensors. RoeFo, submitted, (2009)
[11] M. Helbig, M.A. Hein, U. Schwarz, J. Sachs, Preliminary investigations of chest surface identification algorithms for breast cancer detection, Proc. ICUWB 2008, vol. 2, pp. 195–198, (2008.)
[12] M. Helbig, C. Geyer, M. Hein, I. Hilger, U. Schwarz, J. Sachs, A breast surface estimation algorithm for UWB microwave imaging, in Proc. EMBEC, pp. 760–763, (2008).
[13] M. Lazebnik et al., A large-scale study of the ultrawideband microwave dielectric properties of normal, benign and malignant breast tissues obtained from cancer surgeries, Phys. Med. Biol., vol. 52, pp. 6093–6115, (2007).
[14] X. Li, S. C. Hagness, B. D. Van Veen, and D. van der Weide, Experimental Investigation of Microwave Imaging via Space-Time Beamforming for Breast Cancer Detection, IMS, vol. 1, pp. 379–382, (2003)
[15] T. Sakamoto and T. Sato, A target shape estimation algorithm for pulse radar systems based on boundary scattering transform. IEICE Trans Commun, E87-B:1357–1365, (2004)
[16] M. Helbig, C. Geyer, M. Hein, R. Herrmann, I. Hilger, U. Schwarz, J. Sachs, Improved Breast Surface Identification for UWB Microwave Imaging, IUPESM, WC 2009, Munich, (2009)
[17] U. Schwarz, M. Helbig, J. Sachs, R. Stephan and M. Hein, Design and application of dielectrically scaled double-ridged horn antennas for biomedical UWB radar applications, Proc. ICUWB, (2009).
[18] M.A. Hein, C. Geyer, M. Helbig, I. Hilger, J. Sachs, U. Schwarz, F. Seifert, R. Stephan, and F. Thiel, Antennas for Ultra-Wideband Medical Sensor Systems, EuCAP, pp. 1868–1872, (2009)

First Author
Dr. Florian Thiel, Dr. F. Seifert
Physikalisch-Technische Bundesanstalt (PTB)
Abbe-Str. 2–12, 10587 Berlin, Germany
E-mail: florian.thiel@ptb.de

Prof. Dr. M. A. Hein, Dr. J. Sachs,
Dr. M. Helbig and U. Schwarz
Institute for Information Technology, Ilmenau University of Technology, P.O. Box 100565, Ilmenau, Germany
Prof. Dr. W. A. Kaiser, Prof. Dr. I. Hilger, C. Geyer and G. Rimkus
Institute for Diagnostic and Interventional Radiology, University Hospital Jena,Erlanger Allee 101, 07747 Jena, Germany

This work was supported by the German Research Foundation (DFG) in the UKoLoS priority program (SPP1202, project acronym *ultraMEDIS*).